Electrochimica Acta 91 (2013) 50–57

Contents lists available at SciVerse ScienceDirect

Electrochimica Acta

journal homepage: www.elsevier.com/locate/electacta

The capacitive properties of amorphous manganese dioxide electrodeposited on different thermally-treated carbon papers

Hua Zhao, Gaoyi Han*, Yunzhen Chang, Miaoyu Li, Yanping Li

Institute of Molecular Science, Key Laboratory of Chemical Biology and Molecular Engineering of Education Ministry, Shanxi University, Taiyuan 030006, China

ARTICLE INFO

Article history:
Received 18 October 2012
Received in revised form
26 December 2012
Accepted 26 December 2012
Available online 3 January 2013

Keywords:
MnO_2
Supercapacitor
Carbon paper
Thermal treatment

ABSTRACT

The surface structure of the commercial carbon paper (CP) has been modified through thermal treatment, and then MnO_2 was electrodeposited on the thermally-treated carbon paper (TTCP) by cyclic voltammetry (CV) method in the phosphate buffer solution (PBS, pH 9.18) containing $KMnO_4$. The obtained samples were characterized by X-ray diffraction (XRD), X-ray photoelectron energy spectroscopy (XPS) and scanning electron microscopy (SEM). The results showed that the phase of the obtained MnO_2 was amorphous, and that the morphology of the MnO_2 deposited on the substrates was influenced strongly by the substrates. The capacitive properties of MnO_2 deposited on the carbon substrates were investigated by CV, galvanostatic charge/discharge, electrochemical impedance spectroscopy technique. It was found that the specific capacitance of MnO_2 deposited on the optimum TTCP can reach to 749 F g^{-1} based on the charge/discharge measurement, which was far larger than that on the CP (345 F g^{-1}).

1. Introduction

Electrochemical capacitors as electrical energy storage devices have attracted a lot of attention in many fields such as hybrid power sources, peak power sources and lightweight electric fuse and so on [1–3] due to their greater power density, higher energy density and longer cycle life [4,5]. Based on the operating mechanisms, electrochemical capacitor can be generally classified into two kinds: one is the double-layer capacitors which depend on the charge-separation at the larger surface of the materials of electrode/electrolyte interface; the other is pseudocapacitors which depend on the Faradic redox reaction of the electrochemically active materials. The materials used in pseudocapacitors usually include metal oxides and conducting polymers. Among the metal oxides, manganese oxide is one of the most promising materials of electrode used in electrochemical capacitors because of its low cost, satisfactory capacitive behavior and environmental compatibility.

Up to date, many methods including co-precipitation [6], thermal decomposition [7], sol–gel process [8,9], hydrothermal process [10,11] and electrodeposition [12–18] have been developed to prepare manganese oxides for applications in capacitors. Electro-synthesis is a very promising method for fabrication of thin oxide films for catalytic, electrochemical and biomedical applications because of the easy deposition on substrates without further separation. The process of electrodeposition includes anodic synthesis and cathodic synthesis: in anodic deposition, the Mn^{2+} is oxidized into MnO_2 while in the cathodic process MnO_4^- is reduced into MnO_2. The deposition of MnO_2 on different substrates through anodic process has been reported by many literatures [13–17], during which Na_2SO_4 aqueous solution is usually used as electrolyte. However, the deposition of MnO_2 through cathodic process from MnO_4^- is much less than that of anodic process. Recently, Wei et al. [18] have deposited MnO_2 on stainless steel in Na_2SO_4 solution by using the cathodic process, and the specific capacitance (C_{sc}) of MnO_2 is measured to be about 353 F g^{-1}.

It is well known that the manganese oxide exhibits inherent poor electronic conductivity and that the electrolyte is difficult to penetrate into the inner layer of thick films [16]. The specific capacitance of MnO_2 decreases with the increase of the film's thickness and the values of C_{sc} for MnO_2 films reported in literatures [19,20] are usually in the range of 100–300 F g^{-1} except that the very thin films of MnO_2 (~4 μg cm^{-2}) exhibit [21,22] a C_{sc} of 700 F g^{-1}. On the other hand, carbon paper (CP) should be an ideal alternative conductive substrate/electrode for the electrochemical deposition of electrochemically active materials. Indeed, compared with metallic substrate, CP is a kind of synthetically thin, lightweight matrix with a relatively larger surface area because of the porous spaces on the micrometer scale [23]. Using three-dimensional CP as substrate, the hierarchically porous conductive composites derived from CP decorated with carbon nanotubes have been fabricated and the capacitive properties also been investigated [24]. Recently, the needle-shaped MnO_2 has been deposited on carbon fibers [16]

* Corresponding author. Tel.: +86 351 7010699; fax: +86 351 7016358.
E-mail address: han_gaoyis@sxu.edu.cn (G. Han).

0013-4686/$ – see front matter © 2013 Elsevier Ltd. All rights reserved.
http://dx.doi.org/10.1016/j.electacta.2012.12.114

by using manganese acetate as sources material through anodic synthesis, and the C_{sc} of MnO_2 is measured to be about 432 F g^{-1}.

Therefore, it is interesting to deposit MnO_2 films on the CP in order to obtain a larger supporting amount on unit geometric area. However, the properties of CP are influenced strongly by its surface structure and the oxygen-containing functional groups [25]. The surface modification of the carbons can be usually achieved by electrochemical oxidation, cold plasma treatment and chemical oxidations [26–28], but the method of gaseous oxidation shows less structural damage for carbon [29]. In this paper, the surface of CP is modified by thermal treatment in air, and the different thermally-treated carbon papers (TTCP) are used as substrates for the electro-deposition of MnO_2 layer in PBS buffer containing $KMnO_4$. As a result, this study aims to investigate the influence of the thermal treatment in air on the morphologies and the capacitive properties of MnO_2 deposited on carbon substrates.

2. Experimental

2.1. Reagents and materials

The CP (Toray Composites Inc., Japan) were used directly or after thermal treatment. The commercial CP were thermally treated by two methods: one process was that the CP was heated at 550 °C under atmosphere for 6 h in a muffle furnace and the samples were named as MCP; the other was that the CP was treated in a muffle furnace at 550 °C under atmosphere for 1 h firstly, and then in a muffle furnace at 550 °C for 3 h again after being heated at 1200 °C for 2 h in a tube furnace under Ar atmosphere (MTCP). $KMnO_4$ and other reagents were of analytical grade and used without further purification.

2.2. Electrodeposition of the MnO_2 on CP and TTCP

The PBS solution with a concentration of 0.067 M and pH 9.18 was used as electrolyte. The commercial CP and TTCP were cut into rectangular straps with length of 20 mm and width of 3 mm for use. The electrodeposition was carried out on a CHI 660 C electrochemical station by using CV at scan rate of 100 mV s^{-1} using a three electrode system. The PBS solution containing various amounts of $KMnO_4$ was used as electrolyte, the carbon straps fixed on the copper bar were used as working electrodes, and the Pt foil and saturated calomel electrode (SCE) were used as the counter and reference electrodes, respectively. The optimum experimental procedure was chosen as follows: PBS containing 3.0 mg mL^{-1} of $KMnO_4$ was used as the electrolyte, and the mass of MnO_2 deposited on the substrates was kept to be about 0.43 mg cm^2 based on the geometric area (see supporting materials). The MnO_2 deposited on the CP, MCP and MTCP was defined as CP-MnO_2, MCP-MnO_2 and MTCP-MnO_2, respectively.

2.3. Characterization

The morphologies of the samples were observed on a scanning electron microscope (JSM 6701F) and the X-ray diffraction (XRD) patterns were recorded on a Bruker D8 Advance X-ray diffractometer (Cu Ka) in the 2θ range of 10–80°. X-ray photoelectron spectroscopy (XPS) measurements were performed on an American Thermo-VG Scientific ESCALAB 250XPS system with Al Kα radiation as the exciting source, where the binding energies were calibrated by referencing the C 1s peak (284.6 eV) to reduce the sample charge effect.

The CP straps loaded with MnO_2 were held on the copper rods, a plate of platinum and a SCE electrode were used as working, counter and reference electrode, respectively. The electrochemical measurements were carried out on a CHI660C electrochemical station by using 1.0 M Na_2SO_4 aqueous solution as electrolyte. The measurements of CV were performed in a potential range between −0.1 and 0.8 V at different scan rates. The galvanostatic charge/discharge curves were recorded at varying current densities with the cutoff voltage of −0.1 and 0.8 V. The electrochemical impedance spectra (EIS) were recorded at open-circuit potential in the frequency ranged from 100,000 to 0.01 Hz with ac-voltage amplitude of 5 mV.

Table 1
The relative content of the different bonds on the surface of carbon substrates.

Samples	Relative content of different bonds (%)				
	C═C	C—C	C—OR	C═O	COOR
CP	64.83	29.78	3.05	1.38	0.96
MCP	63.69	27.16	4.85	1.93	2.37
MTCP	63.17	27.24	4.26	2.04	3.29

3. Results and discussion

3.1. The characterization of the TTCP

Usually, the CP has been thermally treated to modify its surface properties because of its weak hydrophilic ability. According to the XPS spectra, it can be found that the relative content of oxygen atom on the surface of CP, MCP and MTCP is about 1.5, 2.5 and 7.7%, respectively. This demonstrates that the thermal treatment can increase the content of oxygen on the surface of carbon fibers. The increment of oxygen-containing groups on the surface of the CP will increase the hydrophilic ability of the substrates. It is interesting to find that the content of oxygen atom on the surface of MTCP increases obviously, which may be contributed to the thermal treatment at higher temperature (1200 °C) under Ar atmosphere before the thermal treatment at 550 °C under air.

Based on the high resolution XPS spectra, the curve fitting of the XPS peaks has been performed using Gauss–Lorentzian peak shape after performing a Shirley background correction and the results are shown in Fig. 1. The XPS peaks of C1s with a binding energy of 284.6 and 285.1 eV can be attributed to the C═C and C—C bonds, and the fitted peaks with binding energy of 286.4, 287.6 and 289.2 eV are typically assigned to C—OR, C═O and O═C—OR functional groups (Fig. 1A), respectively, while the peak located at 291.2 eV is usually assigned the satellite peak ($p–p^*$) of carbon [29,30]. Based on the area of the fitted peak, the relative content of the groups on the surface of the substrates is listed in the Table 1. It is clear that the CP exhibits the most of C═C and C—C bond, but the least of the oxygen-containing groups. However, the relative content of oxygen-containing groups such as C—OR, C═O and O═C—OR increases and the content of C—C bond decreases after thermal treatment, indicating that the default of C—C bond in CP can change into oxygen-containing groups during the thermal treatment. Furthermore, the relative content of O═C-OR groups on MTCP surface is the most, which may indicate that the pre-treatment at high temperature is favorable to form the carboxylic group.

As shown in Fig. 1B, it is found that the XPS peaks of the O1s are asymmetrical. The CP shows two fitted peaks: one located at 532.4 eV which is corresponding to the carbonyl oxygen atoms in esters, anhydrides and the oxygen atoms in hydroxyls or ethers, and the other at 534.1 eV which is related to the carboxyl group (Fig. 1B-a) according to the literature [30]. Besides the fitted peaks located at 532.4–532.8 eV and 533.9–534.2 eV which are similar to that of CP, in the O1s XPS spectra of MCP and MTCP, a new fitted peak at 531.1–531.4 eV is observed and assigned to the oxygen atom in C═O groups. From the above results, it can be found that the thermal treatment in air can not only increase the oxygen content of the carbon surface but also change the types of oxygen atoms in the oxygen-containing groups.

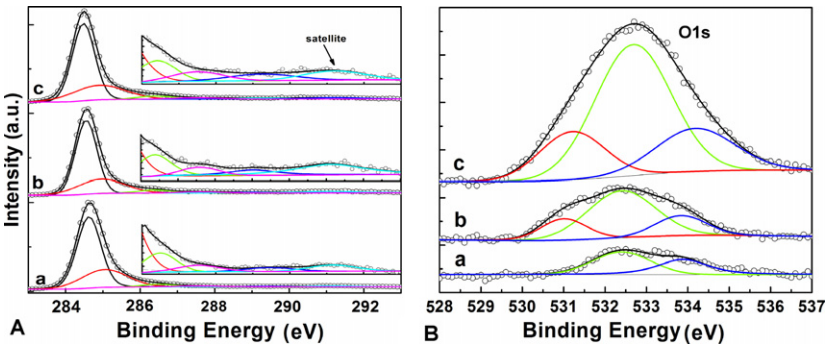

Fig. 1. The XPS peaks of C1s (A) and O1s (B) for CP (a), MCP (b) and MTCP (c).

From the SEM images shown in Fig. 2, it can be found that the surface of fibers in CP is coarse (Fig. 2A), and that many strips and strias are observed on the surface of the fibers. However, the surface of the fibers in MCP becomes smoother than that in CP, moreover, many small particles are observed on the surface, which reveals that the surface of the fibers has been changed by thermal treatment (Fig. 2B). It is interesting to find that the surface of the fibers in MTCP becomes coarse again (Fig. 2C) and is much rougher than that of MCP, and that many small holes and flower-like particles are observed on the surface of the fibers. In order to illustrate the changes of the surface area, the double-layer capacities of the TTCP and CP are also determined in 1.0 mol L^{-1} Na_2SO_4 aqueous solution (Fig. 2D). It can be found that the CV curves are rectangular-like with the almost symmetric *I*–*E* responses for all the electrodes, which are corresponding to the rapid current response on voltage reversal at each end potential and accord with the ideal capacitive behavior. From the current responses at the same condition (the same scan rate and the same geometric area), it can be found that the MTCP exhibits larger surface area than MCP and CP while the surface area of CP is the smallest. The above results reveal that the thermal treatment can change not only the content of oxygen atom but also the surface structure of the fibers.

The XRD pattern of the MTCP shows a sharp diffraction peak at 25.6° which is corresponding to the C (0 0 2) crystal plane. However, it is surprising to find that only the C (0 0 2) peak has appeared in the XRD patterns of CP-MnO_2, MCP-MnO_2 and MTCP-MnO_2 (Fig. 3A), while the diffraction peaks corresponding to MnO_2 do not appear. At the same time, the MnO_2 powder collected from the substrates shows a broad and weak diffraction peak centered at about 26.7°. Based on the above results, it can be deduced that the synthesized MnO_2 is amorphous. In order to clarify the valence state of Mn, the XPS spectra are recorded and shown in Fig. 3B. From the XPS peaks of Mn2p, it is found that the peaks of $Mn2p_{3/2}$ and $Mn2p_{1/2}$ are located at about 642.9 eV and 654.7 eV, the difference between them is about 11.8 eV, indicating that the main product deposited on the carbon substrates is MnO_2 [31]. Furthermore, from the XPS peaks of C1s shown in Fig. 3C, it is found that the MTCP substrate shows the strongest C1s XPS peak, while the sample of MTCP-MnO_2 possesses a weaker XPS peak of C1s than that of MCP-MnO_2. From this phenomenon, it may be deduced that the layer of MnO_2 deposited on MTCP is more continuous and compact than that on the MCP.

The morphologies of MnO_2 deposited on the carbonaceous substrates are observed by SEM and shown in Fig. 4. It can be found

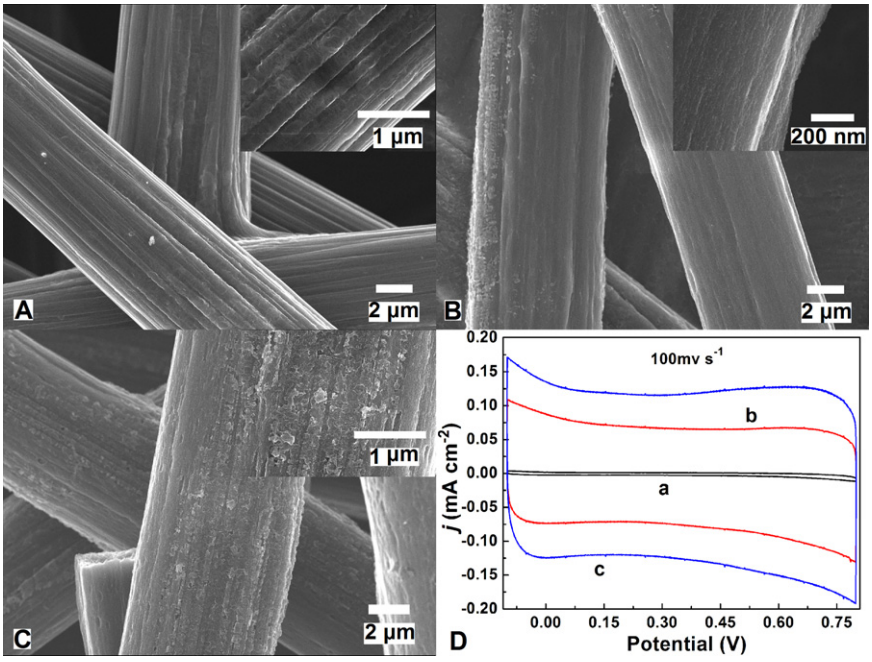

Fig. 2. The SEM images of the commercial CP (A), MCP (B) and MTCP (C), and the CV curves (D) of CP (a), MCP (b) and MTCP (c) in 1.0 M $NaSO_4$ aqueous solution at scan rate of 100 mV s^{-1}.

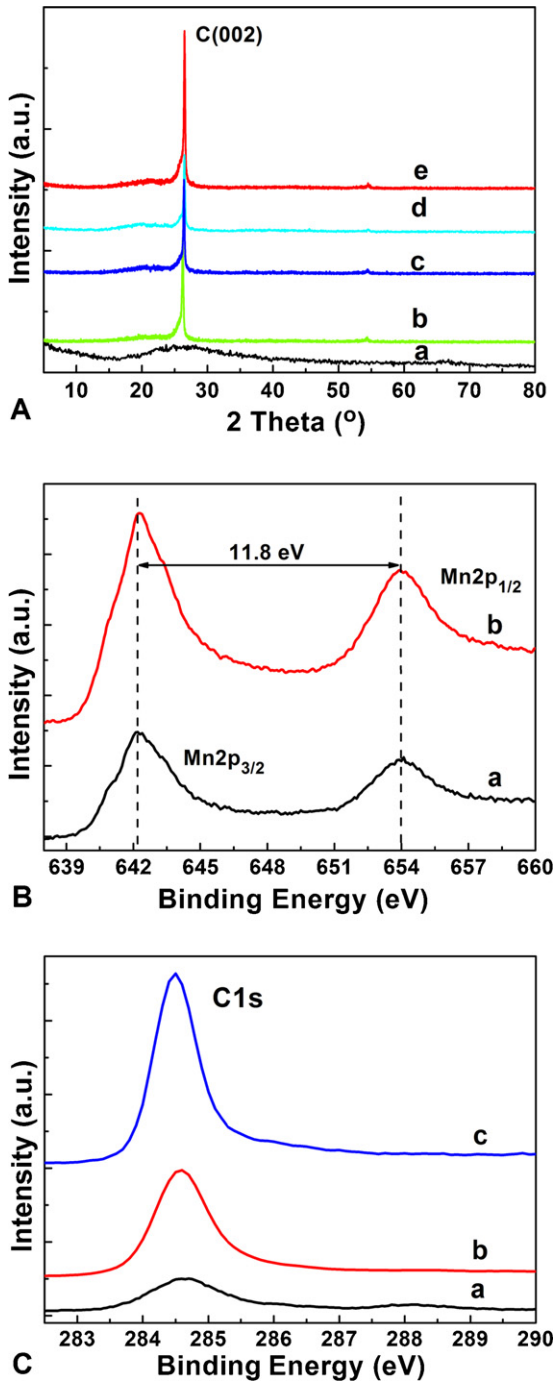

Fig. 3. (A) The XRD patterns of MnO_2 synthesized by CV method (a), CP-MnO_2 (b), MCP-MnO_2 (c), MTCP-MnO_2 (d), and MTCP (e); (B) the Mn2p XPS peaks of MCP-MnO_2 (a) and MTCP-MnO_2 (b); (C) the C1s XPS peaks of MTCP-MnO_2 (a) and MCP-MnO_2 (b) and MTCP (c).

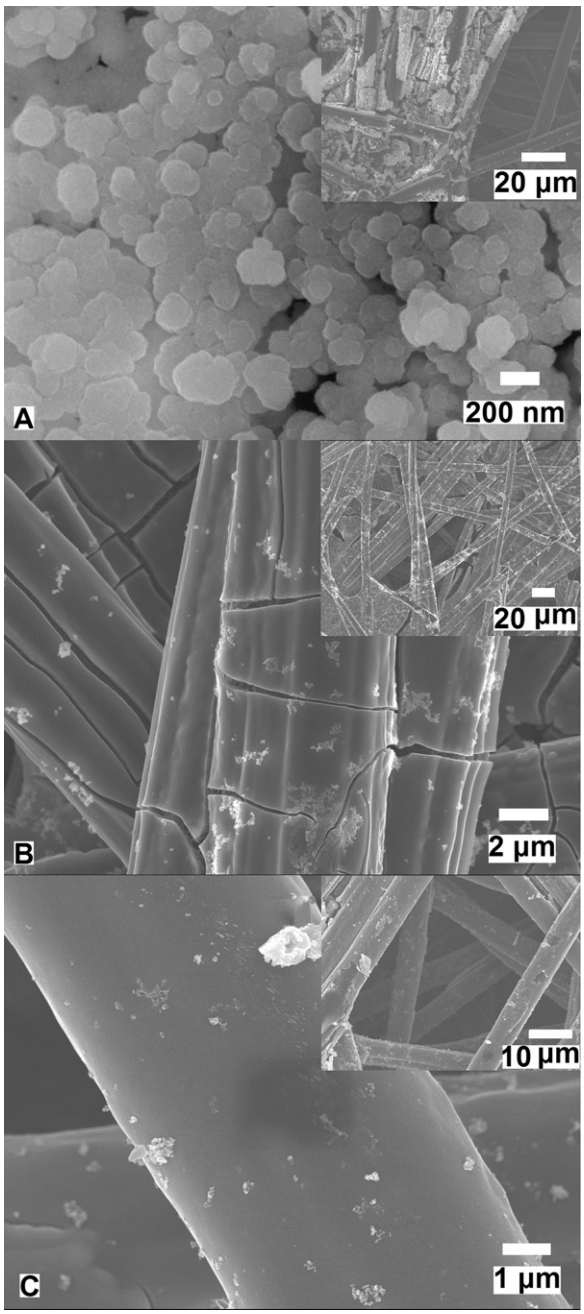

Fig. 4. The SEM images of MnO_2 deposited on (A) CP, (B) MCP and (C) MTCP.

that the MnO_2 particles with irregular shapes are deposited on the CP surface, and that the sizes of the particles are ranged from 100 to 200 nm. From the inserted figure in Fig. 4A, it is clear that the MnO_2 particles are dispersed on the part surface of the CP, and that MnO_2 particles have not been deposited on the inner fibers of the CP. However, it is found that the surface of the fibers in MCP has been covered by a layer of MnO_2 (Fig. 4B) although many cracks are observed on the films. Furthermore, the inner fibers of MCP have been coated with a layer of MnO_2 besides the outer fibers. The thickness of the films deposited on the fibers is measured to be ranged from 210 to 277 nm based on the edge section of the films (see supporting materials). From the Fig. 4C, it is interesting to find that the film deposited on the MTCP is smooth and continuous except that some parts of the films are damaged. Similar to MnO_2 deposited on MCP, the inner and outer fibers of MTCP are coated by the layer of MnO_2. The film's thickness on the MTCP is ranged from 190 to 300 nm (see supporting materials). The above results indicate that the thermal treatment has changed the surface properties of the carbon substrates and that the increase of the content of oxygen-containing group will improve the hydrophilic ability and make the continuous MnO_2 layer form on the surface of carbon fibers. It also illustrates that the XPS peak of C1s for MTCP-MnO_2 is weaker than that of MTCP and MCP-MnO_2 because of the continuous MnO_2 film.

To explore the property of these MnO_2 deposited on carbon substrates as materials of electrochemical capacitor, the electrodes are characterized in 1.0 M Na_2SO_4 electrolyte with CV method because

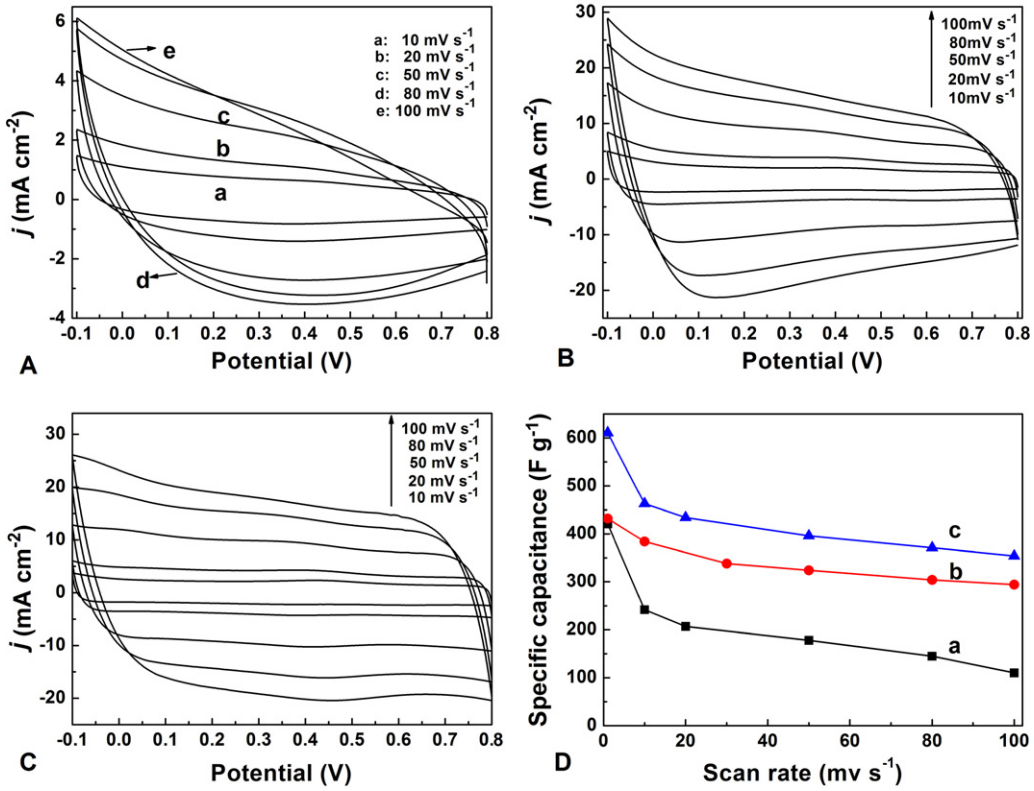

Fig. 5. The CV curves of CP-MnO_2 (A), MCP-MnO_2 (B) and MTCP-MnO_2 (C) at different scan rates in 1.0 M Na_2SO_4 aqueous solution, and the relationship between the specific capacitance and the scan rates (D) for CP-MnO_2 (a), MTCP-MnO_2 (b) and MTCP-MnO_2 (c).

it is a convenient technique to evaluate the capacitive properties. The CV curves recorded at various scan rates from 10 to 100 mV s^{-1} for the samples are shown in Fig. 5A–C. It can be seen that the CV curves of the three electrodes at low scan rate of 10 mV s^{-1} exhibit a symmetrical rectangle-like shape indicating the ideal capacitive behavior. As the scan rate increases, the obvious distortion from the relatively symmetrical rectangle-shape can be observed from the CV curves for the sample of CP-MnO_2. However, it is clear that the distortion from the rectangularity of the CV curves for the sample of MTCP-MnO_2 and MCP-MnO_2 is much less than that for the sample of CP-MnO_2, especially that for MTCP-MnO_2, less distortion from the rectangularity can be observed until the scan rate reaches to 100 mV s^{-1}, indicating much better rate performance due to its finer layer on the carbon fibers.

The C_{sc} (F g^{-1}) of the MnO_2 can be obtained by the following equation:

$$C_{sc} = \frac{Q}{m\Delta E} \quad (1)$$

where Q is the voltammetric charge, ΔE the voltage window (0.9 V), and m the mass of the active material of the electrode. The C_{sc} at different scan rates for the three samples is shown in Fig. 5D. At the scan rate of 1 mV s^{-1}, the sample of MTCP-MnO_2 exhibits a much higher specific capacitance (611 F g^{-1}) than that of MCP-MnO_2 (432 F g^{-1}) and CP-MnO_2 (421 F g^{-1}). The C_{sc} decreases as the scan rate increases, which is typical characteristic for electrochemically active MnO_2 materials. At the highest scan rate of 100 mV s^{-1}, the electrodes of MTCP-MnO_2, MCP-MnO_2 and CP-MnO_2 can maintain 58%, 68% and 26% of their full capacitance (we set the specific capacitance at 1 mV s^{-1} as the full capacitance), respectively. Considering the higher C_{sc} of MTCP-MnO_2, the residual capacity is still far larger than that of MCP-MnO_2 although the MTCP-MnO_2 has a lower remaining percentage for capacity than that of MCP-MnO_2. This result reveals that the thermal treatment of CP can not only increase the C_{sc} but also improve the rate capability of the MnO_2 deposited on it.

Current density is an important factor to determine the capacitive behavior of the as-obtained materials. In order to evaluate the real applicability of our MnO_2 deposited on the carbon substrates, the charge/discharge tests at various current densities are performed and shown in Fig. 6. The C_{sc} can be calculated [4] according to Eq. (2)

$$C_{sc} = \frac{I\Delta t}{m\Delta V} \quad (2)$$

where I is the charge/discharge current density with a unit of A g^{-1}, m the mass with a unit of g, Δt the charge or discharge time with a unit of s, and ΔV the potential during the charge or discharge process. Normally, the discharge process is used to estimate the C_{sc} value. Therefore, the C_{sc} values of CP-MnO_2, MCP-MnO_2 and MTCP-MnO_2 are calculated to be about 556, 676 and 749 F g^{-1} respectively at a discharged current density of 1.0 A g^{-1}. The relationship between the C_{sc} and discharged current density is shown in Fig. 6D, it is found that the C_{sc} value decreases with the increment of the current density for all the samples, and that the C_{sc} for the CP-MnO_2, MCP-MnO_2 and MTCP-MnO_2 is about 267, 411 and 467 F g^{-1} at the current density of 10 A g^{-1}. Furthermore, a 37% decrease of the Cs value for MTCP-MnO_2 is observed with the increase of discharge current density from 1 A g^{-1} to 10 A g^{-1}, which is smaller than that of MCP-MnO_2 (39%) and CP-MnO_2 (52%). From the repeated charge/discharge curves (5 A g^{-1}) shown in Fig. 6E, it is also found that the sample of MTCP-MnO_2 exhibits larger C_{sc} value than that of CP-MnO_2 and MCP-MnO_2, and has the smaller deviation from the cutoff potential during the process, which indicates that MTCP-MnO_2 has better capacitive property.

Fig. 7A shows the Nyquist plots for the MnO_2 deposited on the different carbon substrates, a depressed semicircle (Fig. 7B) in the high-frequency range corresponding to the charge-transfer

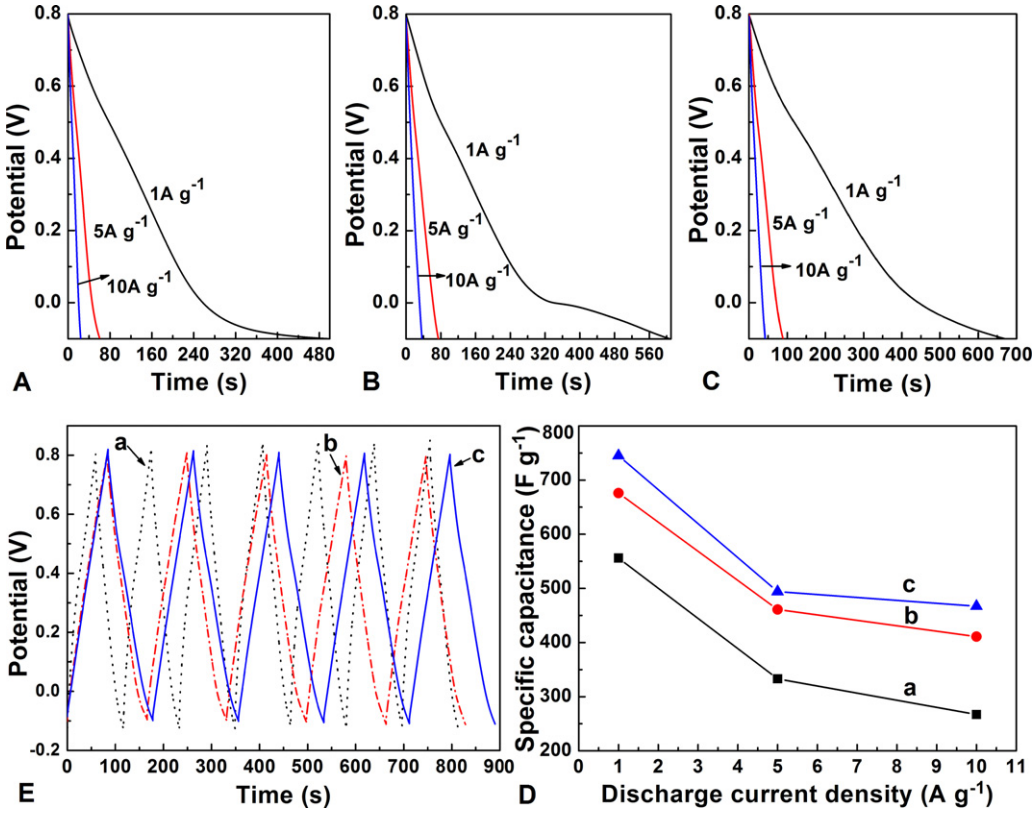

Fig. 6. The discharge curves at different current densities of CP-MnO_2 (A), MCP-MnO_2 (B) and MTCP-MnO_2 (C), and the plots the specific capacitance versus the discharge current densities (D) and the repeated charge/discharge curves (E) for CP-MnO_2 (a), MCP-MnO_2 (b) and MTCP-MnO_2 (c).

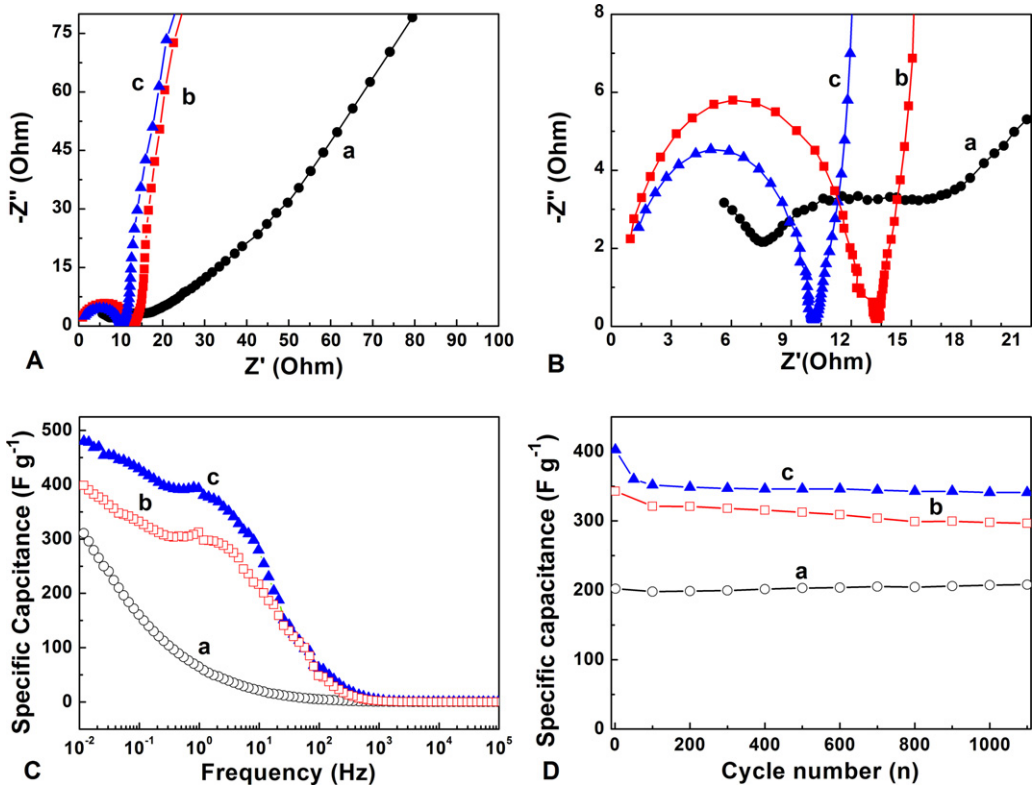

Fig. 7. Nyquist plots (A) and the EIS in high-frequency region (B), the plots of the specific capacitance versus the frequency (C) and the relationships between the specific capacitance and the cyclic numbers (D) of the electrodes (a) CP-MnO_2, (b) MCP-MnO_2 and (c) MTCP-MnO_2.

resistance, and a straight sloping line in the low-frequency range corresponding to the diffusive resistance. The line in the low-frequency range for CP-MnO_2 exhibits a smaller slope than that for MCP-MnO_2 and MTCP-MnO_2, indicating that CP-MnO_2 has a larger diffusive resistance. However, MTCP-MnO_2 has lower charge transfer resistance and diffusive resistance compared with CP-MnO_2 and MCP-MnO_2, confirming further the superior capacitive behavior of the sample of MTCP-MnO_2 [32].

Fig. 7C presents the C_{sc} obtained from EIS for the electrodes based on the following equation [33]:

$$C_{sc} = -\frac{1}{2\pi m f Z''} \quad (3)$$

Here, C_{sc} is the specific capacitance, f the frequency, Z'' the imaginary part of EIS and m the mass of active material in the cell. The C_{sc} of all the capacitors decreases with the increase of the frequency and behaves like a pure resistance in high-frequency region, which reveals that the electrolyte ions cannot be intercalation/deintercalation into the MnO_2 layer. It is also found that MTCP-MnO_2 exhibits a higher C_{sc} at low frequency range compared with CP-MnO_2 and MCP-MnO_2, which is consistent with the results obtained from CV and charge/discharge data. It should be noted that the specific capacitances values of the capacitor cells at 0.01 Hz are deviated from those obtained from CV and charge/discharge test, which is mainly due to the different testing systems applied.

As the service life is a very important factor for the electrochemical capacitors' electrodes, the stability of the electrodes has been evaluated by using CV method at a scan rate of 50 mV s^{-1} and the results are shown in Fig. 7D. It can be found that the C_{sc} of MnO_2 deposited on CP increases slightly after it decreases initially, but the C_{sc} of MnO_2 deposited on MCP and MTCP decreases with the increase of the cyclic number, and the decreasing rate on MTCP is fast at the beginning but slow later. The C_{sc} retains 86.3% and 84.8% of the initial capacitance for MnO_2 deposited on MCP and MTCP after 1100 cycles respectively. Considering the fact that the MnO_2 deposited on the MTCP exhibits the largest C_{sc}, the retained value of capacitance is far larger than that on CP and MCP although only 84.8% of the specific capacitance is retained.

4. Conclusions

The amorphous MnO_2 has been deposited on the TTCP through CV method in the PBS solution containing $KMnO_4$. The morphology and capacitive properties of MnO_2 are influenced strongly by the substrates. The MnO_2 deposited on the MTCP substrate exhibits a C_{sc} of 749 F g^{-1} based on the charge/discharge measurement. The electrochemical measurements also show that the MnO_2 deposited on MTCP possesses a high stability and excellent capacitive properties at high scan rate.

Acknowledgments

The authors thank the National Natural Science Foundation of China (21274082 and 21073115), the Program for New Century Excellent Talents in University (NCET-10-0926) of China and the Program for the Top Young and Middle-aged Innovative Talents of Shanxi province (TYMIT).

Appendix A. Supplementary data

Supplementary data associated with this article can be found, in the online version, at http://dx.doi.org/10.1016/j.electacta.2012.12.114.

References

[1] B.E. Conway, Transition from"supercapacitor" to "battery" behavior in electrochemical energy storage, Journal of the Electrochemical Society 138 (1991) 1539.
[2] M. Ishikawa, M. Morita, M. Ihara, Y. Matsuda, Electric double-layer capacitor composed of actived carbon fiber cloth electrodes and solid polymer electrodes containing alkylammonium salts, Journal of the Electrochemical Society 141 (1994) 1730.
[3] J.P. Zheng, J. Huang, T.R. Jow, The limitations of energy density for electrochemical capacitors, Journal of the Electrochemical Society 144 (1997) 2026.
[4] L. Zhang, G.Q. Shi, Preparation of highly conductive graphene hydrogels for fabricating supercapacitors with high rate capability, Journal of Physical Chemistry C 115 (2011) 17206.
[5] J.K. Chang, C.H. Huang, W.T. Tsai, M.J. Deng, I.W. Sun, P.Y. Chen, Manganese films electrodeposited at different potentials and temperatures in ionic liquid and their application as electrode materials for supercapacitors, Electrochimica Acta 53 (2008) 4447.
[6] H.Y. Lee, V. Manivannan, J.B. Goodenough, Electrochemical capacitors with KCl electrolyte, Comptes rendus Chimie 2 (1999) 565.
[7] M. Toupin, T. Brousse, D. Belanger, The influence of microstructure on the charge storage properties of chemically synthesized manganese dioxide, Chemistry of Materials 14 (2002) 3946.
[8] Y.U. Jeong, A. Manthiram, Nanocrystalline manganese oxides for electrochemical capacitors with neutral electrolytes, Journal of the Electrochemical Society 149 (2002) A1419.
[9] R.N. Reddy, R.G. Reddy, Sol-gel MnO_2 as an electrode material for electrochemical capacitors, Journal of Power Sources 124 (2003) 330.
[10] V. Subramanian, H. Zhu, R. Vajtai, P.M. Ajayan, B. Wei, Hydrothermal synthesis and pseudocapacitance properties of MnO_2 nanostructures, Journal of Physical Chemistry B 109 (2005) 20207.
[11] V. Subramanian, H. Zhu, B. Wei, Nanostructured MnO_2: hydrothermal synthesis and electrochemical properties as a supercapacitor electrode material, Journal of Power Sources 159 (2006) 361.
[12] C.C. Hu, T.W. Tsou, Ideal capacitive behavior of hydrous manganese oxide prepared by anodic deposition, Electrochemistry Communications 4 (2002) 105.
[13] J.K. Chang, W.T. Tsai, Material characterization and electrochemical performance of hydrous manganese oxide electrodes for use in electrochemical pseudocapacitors, Journal of the Electrochemical Society 150 (2003) A1333.
[14] J.K. Chang, W.T. Tsai, Effects of temperature and concentration on the structure and specific capacitance of manganese oxide deposited in manganese acetate solution, Journal of Applied Electrochemistry 34 (2004) 953.
[15] S.L. Chou, J.Z. Wang, S.Y. Chew, H.K. Liu, S.X. Dou, Electrodeposition of MnO_2 nanowires on carbon nanotube paper as free-standing, flexible electrode for supercapacitors, Electrochemistry Communications 10 (2008) 1724.
[16] M.S. Wu, Z.S. Guo, J.J. Jow, Highly regulated electrodeposition of needle-like manganese oxide nanofibers on carbon fiber fabric for electrochemical capacitors, Journal of Physical Chemistry C 114 (2010) 21861.
[17] Q. Cheng, J. Tang, J. Ma, H. Zhang, N. Shinya, L.C. Qin, Graphene and nanostructured MnO_2 composite electrodes for supercapacitors, Carbon 49 (2011) 2917.
[18] J. Wei, N. Nagarajan, I. Zhitomirsky, Manganese oxide films for electrochemical supercapacitor, Journal of Materials Processing Technology 186 (2007) 356.
[19] C.C. Hu, T.W. Tsou, The optimization of specific capacitance of amorphous manganese oxide for electrochemical capacitors using experimental strategies, Journal of Power Sources 115 (2003) 179.
[20] J. Wei, I. Zhitomirsky, Electrosynthesis of manganese oxide films, Surface Engineering 24 (2008) 40.
[21] S.C. Pang, M.A. Anderson, T.W. Chapman, Novel electrode materials for thin-film ultracapacitors: comparison of electrochemical properties of sol-gel-derived and electrodeposited manganese dioxide, Journal of the Electrochemical Society 147 (2000) 444.
[22] S.C. Pang, M.A. Anderson, Novel electrode materials for electrochemical capacitors: Part II. Material characterization of sol-gel-derived and electrodeposited manganese dioxide thin films, Journal of Materials Research 15 (2002) 2096.
[23] T. Bordjiba, M. Mohamedi, L.H. Dao, B. Aissa, M.A.E. Khakani, Enhanced physical and electrochemical properties of nanostructured carbon nanotubes coated microfibrous carbon paper, Chemical Physics Letters 441 (2007) 88.
[24] T. Bordjiba, M. Mohamedi, L.H. Dao, Binderless carbon nanotube/carbon fibre composites for electrochemical micropower sources, Nanotechnology 18 (2007) 35202.
[25] C.T. Hsieh, W.Y. Chen, Y.S. Cheng, Influence of oxidation level on capacitance of electrochemical capacitors fabricated with carbon nanotube/carbon paper composites, Electrochimica Acta 55 (2010) 5294.
[26] Z.R. Yue, W. Jiang, L. Wang, S.D. Gradner, C.U. Pittman Jr., Surface characterization of electrochemically oxidized carbon fibers, Carbon 37 (1999) 1785.
[27] M. Ishikawa, A. Sakamoto, M. Morita, Y. Matsuda, K. Ishida, Effect of treatment of activated carbon fiber cloth electrodes with cold plasma upon performance of electric double-layer capacitors, Journal of Power Sources 60 (1996) 233.
[28] Y.R. Nian, H. Teng, Nitric acid modification of activated carbon electrodes for improvement of electrochemical capacitance, Journal of the Electrochemical Society 149 (2002) A1008.
[29] T.I.T. Okpalugo, P. Papakonstantinou, H. Murphy, J. McLaughlin, N.M.D. Brown, High resolution XPS characterization of chemical functionalised MWCNTs and SWCNTs, Carbon 43 (2005) 153.

[30] U. Zielke, K.J. Huttinger, W.P. Hoffman, Surface-oxidized carbon fibers: I. Surface structure and chemistry, Carbon 34 (1996) 983.
[31] S.W. Lee, J.Y. Kim, S. Chen, P.T. Hammond, Y.S. Horn, Carbon nanotube/manganese oxide ultrathin film electrodes for electrochemical capacitors, ACS Nano 4 (2010) 3889.
[32] M. Inagaki, H. Konno, O. Tanaike, Carbon materials for electrochemical capacitors, Journal of Power Sources 195 (2010) 7880.
[33] M. Jin, G.Y. Han, Y.Z. Chang, H. Zhao, H.Y. Zhang, Flexible electrodes based on polypyrrole/manganese dioxide/polypropylene fibrous membrane composite for supercapacitor, Electrochimica Acta 56 (2011) 9938.